*Desalination and Water Treatment*
www.deswater.com

doi:10.5004/dwt.2017.20983

83 (2017) 193–203
July

# Techno-economic and environmental analysis of an integrated solar vacuum membrane distillation system for the treatment of reverse osmosis desalination brine

Z. Triki[a,*], M.N. Bouaziz[a], M. Boumaza[b]

[a]*Laboratory of Biomaterials and Transport Phenomena, Department of Process and Environmental Engineering, University of Médéa, Médéa 26000, Algeria, Tel./Fax +213 (0) 25 78 52 53, email: triki.zakaria@univ-medea.dz*
[b]*Department of Chemical Engineering, College of Engineering, King Saud University, Riyadh 12372, Saudi Arabia*

Received 24 December 2015; Accepted 21 February 2017

**ABSTRACT**

Reverse osmosis (RO) desalination is widely used for drinking water production, because of its relatively low energy consumption. However, RO is limited in recovery ratio due to the osmotic pressure which increases with salinity. It results with high rejected brine volume inducing negative environmental impact. The aim of this work is to investigate the possibility of using solar vacuum membrane distillation (VMD) in an integrated RO desalination process in order to reduce brine discharge volume and increase RO global recovery ratio. A small RO desalination unit operated by solar energy in a real site in the Algerian desert is considered for the feasibility study. The obtained results proved that important permeate fluxes can be reached with RO coupled with VMD as the water recovery increased from 37% to nearly 87.5%. Brine volume can so be reduced by a factor of 5 and the global water production is more than doubled. A sensitivity analysis was also carried out to study the effects of operating conditions on the desalination system performance in terms of feed water temperature, vacuum pressure and solar collector efficiency. Finally, an economic study was performed to estimate the cost of water produced from the three possible configurations: the RO alone, the VMD alone and the RO-VMD combined system.

*Keywords:* Reverse osmosis desalination; Brine disposal; Vacuum membrane distillation; Solar energy; Economic study; Sensitivity analysis

## 1. Introduction

Drinking water is an essential need for human beings and its production has become a worldwide concern. As the global population continues to grow and develop, the need of potable water is increasing, whereas the availability of natural resources is diminishing. For most, solutions such as water conservation and water transfer or dam construction are not sufficient methods to cope with increasing demand and, in many cases, decreasing supply. Traditional fresh water resources such as lakes, rivers, and groundwater are overused or misused; as a result, these resources are either diminishing or becoming saline [1]. Process technologies for the treatment of saline water are consequently gaining importance and are being developed at a rapid pace. Conventional desalination processes are broadly divided into two main categories, those which are based on the solvent phase change, e.g., distillation and freezing, and those which utilize semi-permeable membranes, e.g., reverse osmosis (RO) and electro-dialysis (ED) [2].

In recent years, RO technology has grown rapidly in desalination plants due to its capability to produce water with relatively less energy consumption compared to thermal desalination technologies. However, the main drawbacks of this technology are the limited recovery and the environmental impact of the rejected brines. Conventional management of RO concentrates, for example traditional solar evaporation, have several disadvantages such as extensive land use and low productivity. Thus, investiga-

*Corresponding author.

*Presented at the 5th Maghreb Conference on Desalination and Water Treatment — CMTDE 2015, December 21–24, 2015, Hammamet, Tunisia*

tion on new options to improve the management of RO concentrates is a current demand [3].

A number of technologies have been studied to improve water recovery and to reduce brine volumes and disposal such as dew vaporation, vibratory shear enhanced membrane filtration process, forward osmosis (FO) and membrane distillation (MD) [4]. FO and MD have been proved to be effective in the recovery of high salt concentration because they are not only less complex; but also enable sustainable energy consumption [5]. An innovative approach was proposed in the frame of the European MEDINA (MEmbrane-based Desalination : an Integrated Approach) project [6] in order to reduce the volume of brines and to increase recovery. It is based on a combination of RO and vacuum membrane distillation (VMD).

VMD is a desalination technology that integrates both thermal distillation and membrane processes. Compared to the other MD configurations, VMD has been proved to be the most energy efficient due to its insignificant temperature polarization effect, relatively high mass flux and energy efficiency [7,8]. One of the most important benefits provided by VMD is the possibility of harnessing available renewable energy sources such as solar energy to supply the heat energy requirement which represents more than 90% of the total energy requirement [9]. Thus, integrating VMD with a solar thermal energy system could compete with an RO process [10].

Very few studies on coupling solar energy with VMD configuration have been reported in the literature. Wang et al. [11] were among the first to couple VMD with solar energy. Polypropylene (PP) hollow fiber membrane module with membrane area of 0.09 $m^2$, an external condenser, a vacuum pump and a solar collector of 8 $m^2$ as a heat source were employed. It was observed that the power consumption of the vacuum pump and the feed circulation pump are much lower than the heat power consumption, especially for high permeate fluxes. A high water production of 32.19 $L{\cdot}m^{-2}{\cdot}h^{-1}$ with a total power consumption of 21.69 kW was reported.

Zhang et al. [12] anticipated the same solar thermal collector to be equipped with VMD to heat lignocellulosic hydrolyzates through a heat exchanger for a concentration purpose. A hollow-fiber polyvinylidene (PVDF) membrane module, with an average pore diameter and porosity of 0.18 μm and 85%, respectively, was used. The consequence of this work articulated that a permeation flux of 8.46 $L{\cdot}m^{-2}{\cdot}h^{-1}$ and rejection of glucose of 99.5% have been outputted at feed temperature of 65°C and feed velocity of 1.0 $m{\cdot}s^{-1}$.

Mericq et al. [13] studied the possibility of submerging the plate VMD membrane in the salinity gradient solar ponds and the solar collector. The use of solar collector does not only seem to be the most interesting solution but also allows a maximum permeate flux of 142 $L{\cdot}m^{-2}{\cdot}h^{-1}$ to be reached with permeable membrane.

Frikha et al. [14] developed a model describing the operation of an autonomous solar VMD unit for seawater desalination. Their model determined the performance of the unit over time and for any day of the year. Simulation results showed that the pilot plant is able to provide average permeate flow rate ranging from 8 to 14 $kg{\cdot}m^{-2}{\cdot}h^{-1}$ on the basis of the sunny period of the day.

Later, Ben Abdallah et al. [15] studied the effect of coupling solar energy with VMD module on the permeate stream for seawater desalination. An improvement has been fulfilled in the daily water production, achieving 49 kg at a vacuum pressure of 1 kPa, with the solar collector coupled with a hollow fiber PVDF membrane module.

Also, an experimental work has been successfully performed by Chafidz et al. [16] for providing potable water in arid remote areas in Saudi Arabia. Solar thermal collector and solar photovoltaic (PV) systems have been used as heat sources for vacuum multi-effect membrane distillation (V-MEMD) module. The results exhibited that about 99.6 L/day drinkable water produced at feed flow rate of 69 $L{\cdot}h^{-1}$ and initial tank temperature of 72°C.

Recently, Wang et al. [17] investigated experimentally the performance of a solar desalination system coupling a vacuum tube solar collector and a VMD unit. The VMD unit used was first tested and examined using an electric heater, and then using the solar collector heater, as a combined system. It was revealed that hot feed temperatures higher than 65°C and cold-side absolute pressure lower than 0.02 MPa are favorable for high trans-membrane flux. The average trans-membrane flux was around 4 $kg\ m^{-2}{\cdot}h^{-1}$ and the specific heat consumption around 750 $kWh/m^3$.

The aim of this paper is to study the feasibility of coupling solar VMD with RO as a complementary process in order to improve the productivity of the desalination system, reducing both energy consumption of the whole system and the discharged brine to a lower environmental impact. A small solar PV-RO desalination unit installed by the CDER (Centre de Développement des Energies Renouvelables) [18] in the village of Hassi-Khebi (southwest of Algeria), is selected in the present work. This unit produces nearly 1000 L/h of fresh water from underground brackish water.

## 2. System description

The solar RO desalination unit of Hassi-Khebi (Fig. 1) includes the following items: RO unit; PV generator; Energy storage and regulation system; Raw and fresh water storage system.

The main components of the RO unit are: the filtration pre-treatment system, the high pressure (HP) pump, six (06) RO modules in series, post-treatment system and accessories. The PV generator is composed of 72 panels with a slope of 35° providing 2.59 kW peak. A control and energy storage system composed of 60 batteries with a total capacity of 500 Ah at 120 V, allows an autonomy of about 3 days. The water storage system includes two tanks of 8 $m^3$ each: one for the raw water and the other for drinking water. In order to prevent formation of calcium sulfate scale, injection of polyacrylates (COATEX EM 201 ASP) has done by chemical dosing pump (2ppm) owing to their good dispersion quality.

The operating conditions of the solar RO desalination unit of Hassi-Khebi are summarized in Table 1.

The main characteristics of the underground brackish water are reported in Table 2.

The solar VMD plant (Fig. 2) consists mainly of flat plate thermal collector, PV panels, lead-acid batteries, heat exchanger, hollow fiber membrane modules, vacuum pump and feed circulation pump.

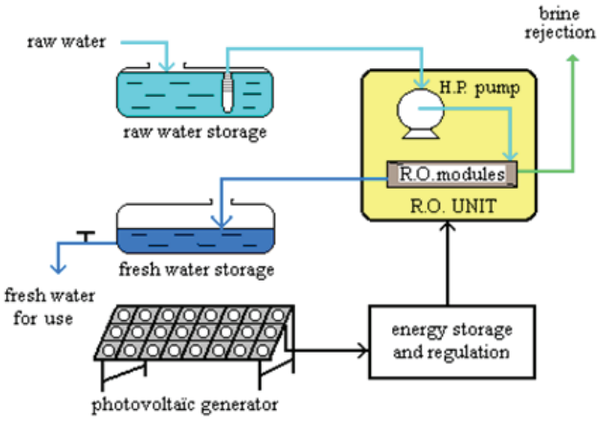


Fig. 1. Schematic diagram of the PV-RO desalination unit [18].

Table 1
Operating conditions of the PV-RO desalination unit [19]

| | |
|---|---|
| Feed flow rate (L/h) | 2575 |
| Product flow rate (L/h) | 950 |
| Feed water temperature (°C) | 26 |
| Feed water salinity (ppm) | 3300 |
| Recovery rate (%) | ~37 |
| Power consumption (kW) | 1.77 |
| Specific energy consumption (kWh/m$^3$) | 1.86 |
| Daily operating time (h) | 6 |
| Daily average radiation (W/m$^2$) | 6790.5 |
| Water production cost ($/m$^3$) | 6 |

Table 2
Characteristics of the feed brackish water

| | |
|---|---|
| T (°C) | 26 |
| pH | 7.9 |
| TDS (ppm) | 3300 |
| $Cl^-$ (ppm) | 1200 |
| $NO_3^-$ (ppm) | 20 |
| $F^-$ (ppm) | 1.1 |
| $SO_4^{2-}$ (ppm) | 502 |
| $Ca^{2+}$ (ppm) | 384 |
| $Na^+$ (ppm) | 584 |
| $HCO_3^-$ (ppm) | 237 |

The membrane chosen in this study is a flat sheet hydrophobic micro-porous Polytetrafluoroethylene (PTFE) membrane (Millipore), because of its high hydrophobicity and excellent resistance towards harsh operation conditions. The typical characteristics of the membrane are summarized in Table 3.

Due to the natural fluctuations of solar radiation, a temporary battery storage is used to avoid energy fluctuations in the system and to enable continuous operation. The permeate side of the hollow fiber module is connected to a vacuum pump to provide the driving force for permeation, and the permeate vapor is condensed and collected in a cold trap immersed in liquid nitrogen.

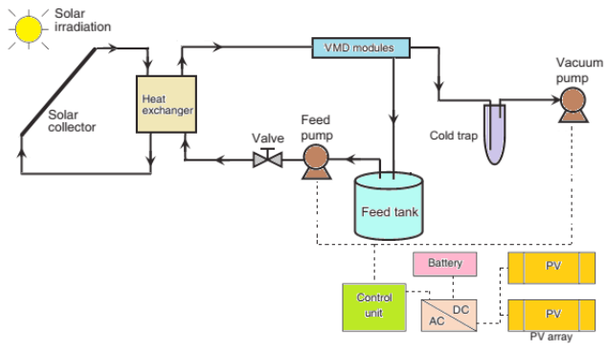


Fig.2. Schematic diagram of the solar VMD plant.

Table 3
VMD membrane characteristics [8]

| | |
|---|---|
| Material | Hydrophobic PTFE |
| Nominal pore size (µm) | 0.22 |
| Thickness (µm) | 175 |
| Porosity (%) | 70 |
| Tortuosity (–) | 1.6 |
| Membrane area (cm$^2$) | 360 |
| Permeability at 293.15 K (s mol$^{1/2}$ m$^{-1}$ kg$^{-1/2}$) | $4.7 \times 10^{-6}$ |

The vacuum pump used in the VMD plant is a single-stage rotary vane mechanical pump that offers an excellent ultimate pressure of 0.02 mbar. These pumps are commonly used for many vacuum distillation and manifold (Schlenk line) applications. Technical specifications of the vacuum pump are given in the Table 4.

The simplified flow diagram of the RO-VMD integrated system is illustrated in Fig. 3. The reject brine from RO is used as the feed solution for VMD. Since the VMD process is far less influenced by salt concentration than RO, more fresh water can be produced and the RO brine volume can be further reduced leading to lower environmental impact.

## 3. VMD modelling

In VMD, the driving force is maintained by applying a continuous vacuum at the permeate side. The hot feed solution is brought into contact with one side of a hydrophobic micro-porous membrane. Generally in the VMD separation process, the vapor water molecules transfer through the membrane pores is given by the mechanism of Knudsen diffusion where the mean free path of the molecules is very large relative to the average pore [21–24]. Then, molecule-pore wall collisions are dominant in membranes with small pores. In addition, Knudsen diffusion dominates in

Table 4
Technical specifications of the vacuum pump [20]

| | |
|---|---|
| Model | Welch DuoSeal 1399C-02 |
| Type | Belt-drive vacuum pump |
| Free air displacement (L/min) | 35 |
| Ultimate pressure (mbar) | 0.019 |
| Rotational pump (rpm) | 750 |
| Motor power (W) | 250 |
| Oil capacity (L) | 0.47 |
| Tubing ID inlet (Inches) | 7/16″ |
| Intake nipple thread | 3/4–20 |
| Exhaust nipple thread | 3/4–20 |
| Weight (kg) | 23 |
| Dimensions (cm) | 43 × 22.9 × 25.42 |

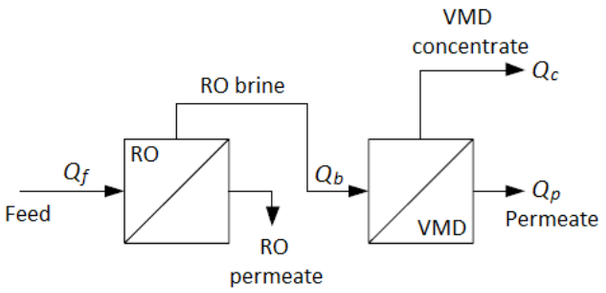


Fig. 3. Flow diagram of RO-VMD integrated system.

VMD if the vacuum is sufficiently pushed. In our case, we used small pore size membrane (0.22 microns) and a very high vacuum does not exceed the 2000 Pa. So the diffusion of the vapor through the membrane pores according to a Knudsen mechanism.

When water is mass transported through the membrane, the molar permeate flux $J_w$ is expressed as follows [6,25]:

$$J_w = \frac{K_M}{\sqrt{M_w}}\left(\alpha_w X_w P_m\left(T_m\right) - P_p\right) \tag{1}$$

where $X_w$ and $M_w$ are respectively the molar fraction and the molar mass of water.

Membrane Knudsen permeability coefficient, $K_M$ is related to membrane properties and it is determined by experiments:

$$K_m = \frac{2}{3}\frac{\varepsilon r}{\tau\delta RT_m}\sqrt{\frac{8RT_m}{\pi}} \tag{2}$$

where $r$ is the pore radius, ε is the porosity, δ is the membrane thickness and τ is the pore tortuosity.

The water activity coefficient, $\alpha_w$ is determined using the correlation equation [21]:

$$\alpha_w = 1 - 0.5X_s - 10X_s^2 \tag{3}$$

The partial vapor pressure at the membrane temperature $T_m$ can be estimated using the Antoine equation [26]:

$$P_m\left(T_m\right) = 133.3 \times 10^{(8.10765-(1750.286/T_m+235))} \tag{4}$$

The water permeate flux is given by:

$$q_w = \frac{J_w M_w}{\rho_w} \tag{5}$$

In the VMD process, electrical energy and thermal energy are required for water circulation and phase conversion, respectively. The equation used for heating energy is given by:

$$P_h = \rho_w Q_p C_{p,w}\left(T_m - T_i\right) \tag{6}$$

The electrical energy consumption of the VMD system is evaluated using specific electrical energy consumption (SEEC), which is the electrical energy consumed per volume unit of distillate produced. The SEEC is calculated using the following equation :

$$SEEC = \frac{P_p + P_v}{Q_p} \tag{7}$$

In this work, the pumping energy, $P_p$ is neglected [27]. The vacuum energy, $P_v$ is given by the equation of McCabe [28]. This equation considers isothermal expansion from atmospheric pressure to the permeate-side pressure.

The theoretical power requirement for the vacuum pump is as follows:

$$P_v = \frac{1.97 \times 10^3}{\eta_{vp}} T_w Q_p \ln\frac{P_{atm}}{P_p} \tag{8}$$

## 4. Economic analysis

The total cost for VMD process involves different steps that depend upon the following factors [29]:

- Source water (salinity and quality of feed water);
- Energy sources (both electrical and thermal are used in VMD);
- Plant size and capacity;
- Plant life, amortization or fixed charges;
- Equipment, renewable energy conversion and storage, etc.);
- Capital (VMD process equipment, membrane modules, installation and building, control instrumentation, land or rental, auxiliary equipment, renewable energy conversion and storage, etc.);
- Operation (pretreatment, post-treatment, brine or concentrate disposal, etc.);
- Maintenance (cleaning, membrane replacement, staff or labour, etc.).

The water production cost, WPC can be determined using the following expression:

$$WPC = \frac{C_{\text{total}}}{fQ_{p,d}365} \tag{9}$$

where $f$ is the plant availability and $Q_{p,d}$ the plant capacity.

The total annual cost, $C_{total}$ can be calculated as:

$$C_{total} = C_{fixed} + C_{O\&M} \quad (10)$$

The annual fixed charges, $C_{fixed}$ can be estimated using the following equation:

$$C_{fixed} = aCC \quad (11)$$

The amortization factor, $a$ is given by:

$$a = \frac{i(1+i)^n}{(1+i)^n - 1} \quad (12)$$

where $i$ is the annual interest rate and $n$ is the lifetime of the plant.

The total capital cost, $CC$ is the sum of the direct capital costs and indirect costs:

$$CC = DCC + ICC \quad (13)$$

Direct capital costs, $DCC$ include cost of civil works ($C_{cw}$), cost of intake and pre-treatment ($C_{I/P}$), Cost of pumps ($C_{PP}$), membrane cost ($C_m$), cost of heat exchanger ($C_{HX}$), cost of solar collector ($C_{sc}$), Cost of PV panel ($C_{PV}$) and battery storage ($C_{bat}$).

Indirect capital costs, $ICC$ are equal to 10% of total direct capital costs [30]:

$$ICC = 0.1 \times DCC \quad (14)$$

Annual operational and maintenance costs, $C_{O\&M}$ consist of membrane replacement fees ($C_{m,repl}$), battery replacement fees ($C_{bat,repl}$), operating and spares fees ($C_{sp}$), annual cost for chemicals ($C_{ch}$), annual labour cost ($C_{lb}$) and annual brine disposal cost ($C_{bd}$).

With the data and assumption of the VMD plant described in Table 5, the WPC was calculated by using the equations listed in Table 6. A sample cost calculation is given in Appendix A3.

Table 5
Data, assumptions and operating conditions used in the economical study

| |
|---|
| *Assumptions of the VMD plant* |
| Plant availability ($f$): 90% |
| Plant life ($n$): 20 years |
| Interest rate ($i$): 5% |
| Zero land cost |
| *Specific costs* |
| Membrane: \$90/m$^2$ [30,31] |
| Membrane replacement: 15%/year of membrane cost [30] |
| Chemicals: \$0.018/m$^3$ [31] |
| Spares: \$0.033/m$^3$ [31] |
| Labour: \$0.03/m$^3$ [31] |
| Brine disposal: \$0.015/m$^3$ [31] |
| Heat exchanger: \$2000/m$^2$ [31] |
| Solar collector: \$100/m$^2$ [32] |
| PV panel: \$5/$W_p$ [32] |
| Battery: \$120/kWh [33] |
| Battery replacement: 50%/year of battery cost [34] |
| *Operating conditions* |
| Feed concentration: 5200 ppm |
| Feed water temperature: 60°C |
| VMD recovery ($r$): 80% |
| VMD permeate pressure: 2000 Pa |

## 5. Results and discussion

### 5.1. System production

Fig. 4 shows the influence of operation time on water production rate for the three configurations investigated namely: RO, VMD and RO-VMD integrated system. As expected, the RO-VMD combined system allows an important increase in the desalination plant capacity which can reach a production rate of about 15.65 m$^3$/d. However, a decrease in the productivity is observed after a certain time due to the accumulation of fouling and scaling on the RO membranes surface as a result of membrane fouling mechanisms.

After three (03) months, the recovery ratio and thus the permeate production has further increased because the scale inhibitor dose has been increased during this period in order to obtain long-term performance results and to establish the chemical cleaning frequency needed. It should be mentioned that scaling occurs in VMD process but its impact on the permeate flux is very limited because it is only reversible and can be easily removed by a simple hydraulic washing as indicated in the literature [25].

### 5.2. System performance

Table 7 summarizes a comparison of the performance of the three configurations. As can be seen from this table, the RO-VMD integrated system can produce more than twice as much water as the RO alone. The individual RO recovery was 37%, and VMD recovery was 80%, thus giving a global water recovery of 87.4% for the combined system with a reduction of the quantity of brine produced by a factor of 5. Moreover, the SEEC is reduced by half after coupling RO with solar VMD. This confirm the great opportunity of using solar thermal energy for feed water preheating in order to reduce energy requirement. It is also important to mention that the VMD process had a significantly lower SEEC compared to the RO process (i.e., 0.16 compared to 1.86 kWh/m$^3$). This comparison roughly demonstrates the advantage of VMD over RO for water desalination when integrating with solar energy.

### 5.3. Sensitivity analysis

#### 5.3.1. Effect of feed water temperature

The effect of feed water temperature on permeate flux and system water production cost is shown in Fig. 5. In the

Table 6
Equations for water production cost estimation

| Cost ($) | Equation |
|---|---|
| Direct capital costs | |
| $C_m = 90 \times A_m$ | (15) |
| $A_m = (Q_p / q_w)$ | (16) |
| $C_{cw} = 1945 \times r(Q_{p,d})^{0.8}$ | (17) |
| $C_{(I/P)} = 658 \times r(Q_{(p,d)} / r)^{0.8}$ | (18) |
| $C_{pp} = 1.43 \times 10^{-3}(Q_{p,d} \cdot \Delta P / r)$ | (19) |
| $C_{sc} = 100 \times A_{sc}$ | (20) |
| $A_{sc} = (P_h \times t) / (\eta_{sc} \cdot I_{G,m})$ | (21) |
| $C_{HX} = 2000 \times A_{HX}$ | (22) |
| $A_{HX} = \frac{(P_h / \eta_{HX})}{U \cdot \Delta T_m}$ | (23) |
| $C_{PV} = 5 \times P_{PV}$ | (24) |
| $P_{PV} = (P_v / \eta_{PV} \cdot \eta_{bat} \cdot \eta_{inst})$ | (25) |
| $C_{bat} = 200 \times E_{bat}$ | (26) |
| $E_{bat} = (P_v \cdot N_j \cdot t \cdot k_a \cdot k_t \cdot k_c / 1000 \times k_{dod})$ | (27) |
| $DCC = C_m + C_{cw} + C_{I/P} + C_{pp} + C_{sc} + C_{HX} + C_{PV} + C_{bat}$ | (28) |
| $C_{m,repl} = 0.15 \times C_m$ | (29) |
| $C_{bat,repl} = 0.5 \times C_{bat}$ | (30) |
| $C_{ch} = 365 f Q_{p,d} \times 0.018$ | (31) |
| $C_{sp} = 365 f Q_{p,d} \times 0.033$ | (32) |
| $C_{lb} = 365 f Q_{p,d} \times 0.03$ | (33) |
| $C_{bd} = 365 f Q_{p,d} \times 0.015$ | (34) |
| $C_{O\&M} = C_{m,repl} + C_{bat,repl} + C_{ch} + C_{sp} + C_{lb} + C_{bd}$ | (35) |

Assumptions.
$\eta_{vp} = 0.8$, $\eta_{PV} = 0.15$, $\eta_{bat} = 0.75$, $\eta_{inst} = 0.85$, $\eta_{sc} = 0.5$
$k_a = 1.25$, $k_t = 0.987$, $k_c = 1.1$, $k_{dod} = 0.5$
$\eta_{HX} = 0.8$; $U = 2500$ W/m² K; $\Delta T_m = 40$ K

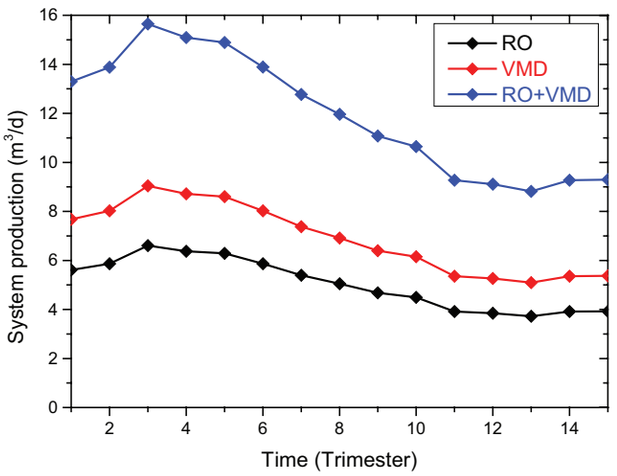


Fig. 4. Time-variation of water production rate for the three configurations.

Table 7
Performance comparison of the three configurations

| Operating conditions | RO | VMD | RO-VMD |
|---|---|---|---|
| Feed flow rate (m³/d) | 15.45 | 9.75 | 15.45 |
| Permeate flow rate (m³/d) | 5.7 | 7.8 | 13.5 |
| Concentrate flow rate (m³/d) | 9.75 | 1.95 | 1.95 |
| Recovery (%) | ~37 | 80 | ~87.4 |
| Electric power consumption (kW) | 1.77 | 0.21 | 1.98 |
| Specific electrical energy consumption (kWh/m³) | 1.86 | 0.16 | 0.88 |

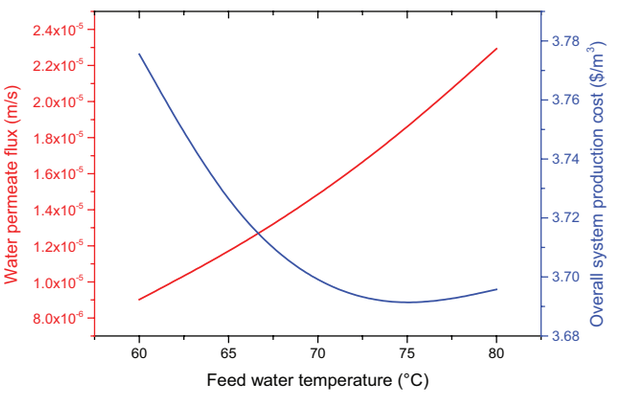


Fig. 5. Effect of feed water temperature on the system performance.

range of studied temperature from 60 to 80°C, the water permeation flux can be increased exponentially by raising the feed temperature as a consequence of the increase in the thermal driving force: the saturated water vapor pressure increase significantly with temperature. Water costs generally decline with increase in temperature as a result of the increase in feed-side water vapor pressure. However, the greater amount of heating energy required at the higher temperatures, increase solar collector cost. As the fixed costs are not associated with heating do not increase, a local minimum cost occurs when the heater cost begins to dominate and drive up the overall system cost. It must be noted that feed water temperature should not exceed 80°C view that the structure of VMD membranes cannot withstand

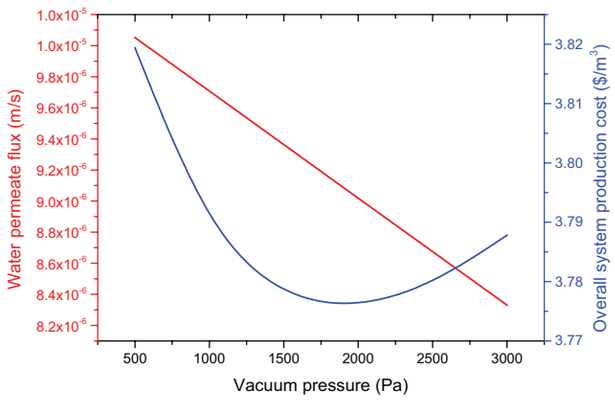


Fig. 6. Effect of vacuum pressure on the system performance.

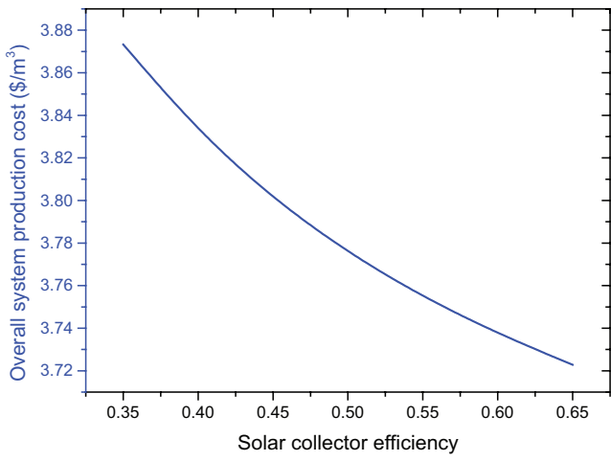


Fig. 7. Effect of solar collector efficiency on the system performance.

high temperatures which can cause an alternation of their mechanical.

### 5.3.2. Effect of vacuum pressure

Fig. 6 shows the effect of vacuum pressure on the system performance. As shown in this figure, the water permeate flux decreased gradually with increasing pressure because of the loss of the driving force across the membrane: the more difference between permeate-side membrane pressure and water saturated vapor pressure at system temperature, the more the driving force of VMD process. Generally, by increasing the degree of vacuum, the WPC decreases due to increase in the permeate flux through the membrane. However, if the pressure becomes too small, the pumping power increases, increasing the PV area needed and driving up the cost for electrical energy for the vacuum pump. The result is a high cost per unit water produced where the cost is dominated by fixed system cost. Therefore, it is preferable to maintain moderate vacuum levels taking into account economic considerations.

### 5.3.3. Effect of solar collector efficiency

The effect of solar collector efficiency on the system water production cost is shown in Fig. 7. As can be seen, collector efficiency has a large impact on water cost. Generally, collectors with higher efficiency have a lower overall production cost. The more efficient a collector the less area is required. However, collector efficiency varies during the day, typically going down with higher top temperature in the collector, which increases losses. Moreover, high-efficiency solar collectors are quite expensive. We note that despite their lower efficiency the flat plate collector presents a low cost compared to other collectors, and it well suited for applications where the temperature levels are moderate such as VMD process.

### 5.4. Economic study:

Water production costs for the three configurations are given in Fig. 8. The estimated WPC for the solar RO desalination unit ($6/m$^3$) is within the same order of magnitude

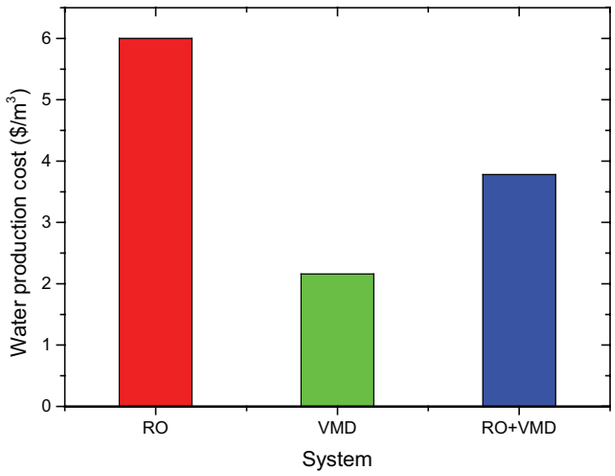


Fig. 8. Estimated water production cost for each configuration.

with that produced from commercial PV-RO process which costs between $2–13/m$^3$ [39]. However, the results show that solar VMD has a better cost effective ($2.16/m$^3$) because, in this case, the solar collector is employed as the main solar energy collection unit and the more expensive PV panel is only used to supply electricity for vacuum pump and circulator. Therefore, the WPC value obtained for the RO-VMD integrated system is found to be economically cost competitive ($3.78/m$^3$) compared to other mature solar-driven desalination systems cited in the literature [40].

## 6. Conclusion

This paper has investigated the possibility of the use of solar VMD operating on the brine of a RO desalination process in order to improve its performance. A small PV-RO unit installed in the village of Hassi-Khebi in the south of Algeria has been chosen for the feasibility study. The results confirmed that VMD can be a very interesting option for treating

RO brine. Indeed, by coupling RO with VMD, high recovery can be obtained (87.4% in this study), corresponding to a brine volume reduction by a 5 factor, while the global water production can be increased by more than 2.

Sensitivity of the RO-VMD desalination system was determined with respect to several parameters such as feed water temperature, vacuum pressure and solar collector efficiency; and the following conclusions can be drawn from the parametric study:

- the increase in feed water temperature significantly increased the permeate flux because of the exponential relationship between the vapor pressure and the temperature. However, the water cost decreased with increasing feed temperature up to a certain critical value after which increasing water temperature resulted in increasing WPC as a penalty of more heating energy is required for the feed, thus, raising the required solar collector area and consequently the cost. Besides, it is worth noting that feed water temperature should not exceed 80°C for the structure of membrane cannot resist high temperatures that can cause an alteration of their mechanical strength.
- the decrease in vacuum pressure increased the water permeation flux due to an increase in VMD driving force. However, the benefit of high water production did not significantly overweighed the electrical cost stemming from the high vacuum, resulting in the choice of a moderate degree of vacuum for the sake of low WPC.
- the increase in the solar collector efficiency decrease WPC by decreased solar collection area. However, collectors that are more efficient are usually more expensive. This results in the need to balance collector cost with efficiency.

Finally, an economic analysis was performed for the three possible configurations: the RO alone, the VMD alone and the RO-VMD combined system. It was found that solar VMD with a WPC of \$2.16/m$^3$ is the most cost effective configuration due to its low SEEC. However, it is important to note that the production cost obtained for the RO-VMD integrated system (\$3.78/m$^3$) is found to be relatively low compared to other mature solar-driven desalination systems reported in literature.

## Nomenclature

$a$ — Amortization factor
$A$ — Area (m$^2$)
$C$ — Cost (\$)
$C_p$ — Heat capacity (J/kg·°C)
$CC$ — Capital cost (\$)
$DCC$ — Direct capital cost (\$)
$f$ — Plant availability (%)
$i$ — Interest rate (%)
$I_{g,m}$ — Average global solar irradiation (W/m$^2$)
$ICC$ — Indirect capital cost
$J_w$ — Water molar permeate flux (mol/s·m)
$k_a$ — Battery aging factor
$k_c$ — Capacity rating factor
$k_{dod}$ — Depth of discharge
$k_t$ — Temperature correction factor
$K_m$ — Membrane permeability (mol$^{1/2}$·s/m·kg$^{1/2}$)
$N_i$ — Days of autonomy (d)
$M_w$ — Water molar mass (kg/mol)
$P$ — Pressure (Pa) power (W)
$q_m$ — Water permeate flux (m/s)
$Q$ — Volumetric flow rate (m$^3$/s)
$Q_{p,d}$ — Plant capacity (m$^3$/d)
$r$ — Membrane pore radius (m)
$R$ — Gas constant (J/mol·K)
$E_{bat}$ — Battery capacity (kWh)
$SEEC$ — Specific electrical energy consumption (kWh/m$^3$)
$t$ — Operating time (h/d)
$T$ — Temperature (°C)
$U$ — Global heat transfer coefficient (W/m$^2$·K)
$v$ — Vacuum
$X_s$ — Salt molar fraction
$X_w$ — Water molar fraction

### Greek letters

$\alpha_w$ — Water activity coefficient
$\Delta$ — Difference
$\delta$ — Thickness (m)
$\varepsilon$ — Pore size (m)
$\eta$ — Efficiency (–)
$\rho$ — Density (kg/m$^3$)
$\tau$ — Tortuosity (–)

### Subscripts

*atm* — Atmospheric
*b* — Brine
*bat* — Battery
*bat,repl* — Battery replacement
*c* — Concentrate
*ch* — Chemical
*f* — Feed
*h* — Heating
*HX* — Heat exchanger
*i* — Initial
*ins* — Installation
*i/p* — Intake and pretreatment
*lb* — Labour
*m* — Membrane
*m,repl* — Membrane replacement
*O&M* — Operation and maintenance
*p* — Permeate, pumping
*pp* — Pump
*PV* — Photovoltaic
*s* — Salt
*sc* — Solar collector
*sp* — Spares
*vp* — Vacuum pump
*w* — Water

### Superscripts

*n* — Plant life

## References


[1] L.F. Greenlee, D.F. Lawler, B.D. Freeman, B. Marrot, P. Moulin, Reverse osmosis desalination: water sources, technology, and today's challenges, Water Res., 43(9) (2009) 2317–2348.

[2] S.T. Bouguecha, A. Boubakri, S.E. Aly, M.H. Al-Beirutty, M.M, Hamdi, Solar driven DCMD: Performance evaluation and thermal energy efficiency, Chem. Eng. Res. Des., 100 (2015) 331–340.

[3] A. Pérez-González, A.M. Urtiaga, R. Ibáñez, I. Ortiz, State of the art and review on the treatment technologies of water reverse osmosis concentrates, Water Res., 46(2) (2012) 267–283.

[4] P. Xu, T. Cath, A.P. Robertson, M. Reinhard, J.O. Leckie, J.E. Drewes, Critical review of desalination concentrate management, treatment and beneficial use, Environ Eng Sci., 30(8) (2013) 502–514.

[5] C.R. Martinetti, A.E. Childress, T.Y. Cath, High recovery of concentrated RO brines using forward osmosis and membrane distillation, J. Membr. Sci., 331(1) (2009) 31–39.

[6] J.-P. Mericq, S. Laborie, C. Cabassud, Vacuum membrane distillation for an integrated seawater desalination process, Desal. Water Treat., 9 (2009) 287–296.

[7] K.W. Lawson, D.R. Lloyd, Membrane distillation. I. Module design and performance evaluation using vacuum membrane distillation, J. Membr. Sci., 120(1) (1996) 111–121.

[8] B. Li, K.K. Sirkar, Novel membrane and device for vacuum membrane distillation based desalination process, J. Membr. Sci., 257(1–2) (2005) 60–75.

[9] M. Khayet, T. Matsuura, Membrane Distillation, Principles and Applications, 1st ed., Elsevier: Kidlington, Oxford, UK, 2011.

[10] N. Couffin, C. Caufin, C. Cabassud, V. Lahoussine-Turcaud, A new process to remove halogenated VOCs or drinking water production: vacuum membrane distillation, Desalination, 117(1–3) (1998) 233–245.

[11] X. Wang, L. Zhang, H. Yang, H. Chen, Feasibility research of potable water production via solar-heated hollow fiber membrane distillation system, Desalination, 247 (2009) 403–411.

[12] L. Zhang, Y. Wang, L.H. Cheng, X. Xu, H. Chen, Concentration of lignocellulosic hydrolyzates by solar membrane distillation, Bioresour. Technol., 123 (2012) 382–385.

[13] J. Mericq, S. Laborie, C. Cabassud, Evaluation of systems coupling vacuum membrane distillation and solar energy for seawater desalination, Chem. Eng. J., 166 (2011) 596–606.

[14] N. Frikha, R. Matlaya, B. Chaouachi, S. Gabsi, Simulation of an autonomous solar vacuum membrane distillation for seawater desalination, Desal. Water Treat., 52 (2014) 1725–1734.

[15] S. Ben Abdallah, N. Frikha, S. Gabsi, Simulation of solar vacuum membrane distillation unit, Desalination, 324 (2013) 87–92.

[16] A. Chafidz, S. Al-Zahrani, M.N. Al-Otaibi, C.F. Hoong, T.F. Lai, M. Prabu, Portable and integrated solar-driven desalination system using membrane distillation for arid remote areas in Saudi Arabia, Desalination, 345 (2014) 36–49.

[17] Y. Wang, Z. Xu, N. Lior, H. Zeng, An experimental study of solar thermal vacuum membrane distillation desalination, Desal. Water Treat., 53 (2015) 887–897.

[18] A. Sadi, S. Kehal, Retrospectives and potential use of saline water desalination in Algeria, Desalination, 152 (2002) 51–56.

[19] A. Maurel, Dessalement de l'eau de mer et des eaux saumâtres [Desalination of seawater and brackish waters], 2nd ed., Tec&Doc, 2006, 286p.

[20] Welch-Ilmvav, Vacuum Pump and Systems, 2011–2012 Catalog, 2011, pp. 32–33. Available: http://pdf.directindustry.com/pdf/welch/ilmvac-vacuum-pump-systems-catalog-2011-2012/14506-237218.html.

[21] K.W. Lawson, D.R. Lloyd, Membrane distillation. Review, J. Membr. Sci., 124 (1997) 1–25.

[22] T.D. Dao, J.P. Mericq, S. Laborie, C. Cabassud, A new method for permeability measurement of hydrophobic membranes in vacuum membrane distillation process, Water Res., 47 (2013) 2096–2104.

[23] M. Abu-Zeid, Y. Zhang, H. Dong, L. Hou, A comprehensive review of vacuum membrane distillation technique, Desalination, 356 (2015) 1–14.

[24] L. Sun, L. Wang, Z. Wang, S. Wang, Characteristics analysis of cross flow vacuum membrane distillation process, J. Membr. Sci., 488 (2015) 30–39.

[25] J.P. Mericq, S. Laborie, C. Cabassud, Vacuum membrane distillation of seawater reverse osmosis brines, Water Res., 44 (2010) 5260–5273.

[26] R.M. Felder, R.W. Rousseau, Elementary Principles of Chemical Processes, 3rd ed., John Wiley & Sons, New York, 2000.

[27] C. Cabassud, D. Wirth, Membrane distillation for water desalination: how to choose an appropriate membrane, Desalination, 157 (2003) 307–314.

[28] W.L. McCabe, J.C. Smith, P. Harriott, Unit operations of chemical engineering, 5th ed., McGraw-Hill, New York, 1993, pp. 1010–1027.

[29] M. Khayet, Solar desalination by membrane distillation: Dispersion in energy consumption analysis and water production costs (a review), Desalination, 308 (2013) 89–101.

[30] F. Macedonio, E. Curcio, E. Drioli, Integrated membrane systems for seawater desalination: energetic and exergetic analysis, economic evaluation, experimental study, Desalination, 203 (2007) 260–276.

[31] S. Al-Obaidani, E. Curcio, F. Macedonio, G.D. Profio, H. Al-Hinai, E. Drioli, Potential of membrane distillation in seawater desalination: thermal efficiency,sensitivity study and cost estimation, J. Membr. Sci., 323 (2008) 85–98.

[32] F. Banat, N. Jwaied, Economic evaluation of desalination by small-scale autonomous solar-powered membrane distillation units, Desalination, 220 (2008) 566–573.

[33] S. Anuphappharadorn, S. Sukchai, C. Sirisamphanwong, N. Ketjoy, Comparison the economic analysis of the battery between lithium-ion and lead-acid in PV stand-alone application, Energy Procedia, 56 (2014) 352–358.

[34] A.M. Helal, A.M. El-Nashar, E. Al-Katheeri, S. Al-Maler, Optimal design of hybrid RO/MSF desalination plants. Part I. Modeling and algorithms, Desalination, 154 (2003) 43–66.

[35] A.M. Helal, A.M. El-Nashar, E.S. Al-Katheeri, S.A. Al-Malek, Optimal design of hybrid RO/MSF desalination plants. Part I: Modeling and algorithms, Desalination, 154 (2003) 43–66.

[36] H.E. Fath, S.M. Elsherbiny, A.A. Hassan, M. Rommel, M. Wieghaus, J. Koschikowski, M. Vatansever, PV and thermally driven small-scale, stand alone solar desalination systems with very low maintenance needs, Desalination, 225(1–3) (2008) 58–69.

[37] R. Sarbatly, C.K. Chiam, Evaluation of geothermal energy in desalination by vacuum membrane distillation, Appl. Energy, 112 (2013) 737–746.

[38] IEEE Recommended Practice for Sizing Lead-Acid Batteries for Stationary Applications. IEEE Std 485-2010, 2011, pp. 1–90.

[39] A. Gharmandi, R. Messalem, Solar-driven desalination with reverse osmosis: the state of the art, Desal. Water Treat., 7 (2009) 285–296.

[40] M.T. Ali, Hassan E.S. Fath, Peter R. Armstrong, A comprehensive techno-economical review of indirect solar desalination, Renew. Sustain. Energy Rev., 15 (2011) 4187–4199.

[41] B.S. Sparrow, Empirical equations for the thermodynamic properties of aqueous sodium chloride, Desalination, 159 (2003) 161–170.

## Appendix A

*A.1. Water density*

Water density, $\rho_w$ is estimated using the empirical equation developed by Sparrow [41]. This equation is valid for temperatures from 0 to 300°C, and concentrations extending to saturation.

$$\rho_w = A + BT_m + CT_m^2 + DT_m^3 + ET_m^4 \quad \text{(A.1)}$$

where:

$$A = \left(1.001 + 0.7666X_s + 0.0149X_s^2 + 0.2663X_s^3 + 0.8845X_s^4\right)\times 10^3$$

$$B = -0.0214 - 3.496X_s + 10.02X_s^2 - 6.56X_s^3 - 31.37X_s^4$$

$$C = \left(-5.263 + 39.87X_s - 176.2X_s^2 + 363.5X_s^3 - 7.784X_s^4\right)\times 10^{-3}$$

$$D = \left(15.42 - 167X_s + 980.7X_s^2 - 2573X_s^3 + 876.6X_s^4\right)\times 10^{-6}$$

$$E = \left(-0.0276 + 0.2978X_s - 2.017X_s^2 + 6.345X_s^3 - 3.914X_s^4\right)\times 10^{-6}$$

*A.2. Specific heat capacity of water*

Specific heat capacity of water, $C_{p,w}$ is expressed as a function of temperature by the quadratic, neglecting salinity effects:

$$C_{p,w} = 5252.4 - 6.9474T_m + 0.0112T_m^2 \quad \text{(A.2)}$$

*A.3. Sample cost calculation for the solar VMD plant*

*A.3.1. Total capital costs*

Water molar permeate flux:

$$J_w = \frac{K_M}{\sqrt{M_w}}\left(\alpha_w X_w P_m\left(T_m\right) - P_p\right) =$$
$$\frac{5.56\times 10^{-6}}{\sqrt{0.018}}\left(0.999\times 0.236\times 15138.94 - 2000\right)$$
$$= 0.543(\text{mol}/\text{s.m}^2)$$

Water permetae flux:

$$q_w = J_w M_w / \rho_w = 0.543\times 0.018 / 1083.668 = 9.019\times 10^{(-6)}\, m/s$$

Required membrane area:

$$A_m = Q_p / q_w = 3.611\times 10^{-4} / 9.019\times 10^{-6} = 40.038 m^2$$

Total cost of membranes:

$$C_m = 90\times A_m = 90\times 40.038 = 3603.481\,\$$$

Cost of civil works:

$$C_{cw} = 1945\times r\left(Q_{p,d}\right)^{0.8}\, 1945\times 0.8\times\left(7.8\right)^{0.8} = 8047.951\$$$

Cost of intake and pretreatment:

$$C_{I/P} = 658\times r(Q_{p,d}/r)^{0.8} = 658\times 0.8\times(7.8./0.8)^{0.8} = 3254.765\$$$

Cost of pumps

$$C_{pp} = 1.43\times 10^{-3}(Q_{p,d}.\Delta P / r) =$$
$$1.43\times 10^{-3}(7.8\times(101325 - 2000)/0.8) = 1384.839\$$$

Heat energy requirement

$$P_h = \rho_w Q_p C_{p,w}\left(T_m - T_i\right) = 1083.668\times 3.611\times 10^{-4}$$
$$\times 4875.879\times(60 - 26) = 64873.71\text{W}$$

Required solar collector area

$$A_{sc} = (P_h\times t)/(\eta_{sc}.I_{G,m}) = (64873.71\times 6)/(0.5\times 6790.5) = 114.64 m^2$$

Cost of solar collector

$$C_{sc} = 100\times A_{sc} = 100\times 114.64 = 11464.32\$$$

Required heat exchanger area

$$A_{HX} = \frac{(P_h/\eta_{HX})}{(U.\Delta T_m)} = \frac{64873.71/0.8}{(2500\times 40)} = = 0.81 m^2$$

Cost of heat exchanger

$$C_{HX} = 2000\times A_{HX} = 2000\times 0.81 = 1621.843\$$$

Power consumption of the vacuum pump

$$P_v = \frac{1.97\times 10^3}{\eta_{vp}} T_w Q_p \ln\frac{P_{atm}}{P_p} = \frac{1.97\times 10^3}{0.8}$$
$$\times 26\times 3.611\times 10^{-4}\times\ln\frac{101325}{2000} = 209.425\text{W}$$

Power output of PV panels

$$P_{PV} = (P_{vp}/\eta_{PV}.\eta_{bat}.\eta_{inst}) = 209.425/0.15\times 0.75\times 0.85 = 2190.066 W$$

Cost of PV panels

$$C_{PV} = 5\times P_{PV} = 5\times 2190.066 = 10950.33\$$$

Capacity of batteries

$$E_{bat} = (P_v.N_j.t.k_a.k_t.k_c)/1000\times k_{dod} =$$
$$(209.425\times 3\times 6\times 1.25\times 0.987\times 1.1)/(1000\times 0.5) = 10.232 kWh$$

Cost of batteries

$$C_{bat} = 200\times E_{bat} = 200\times 10.232 = 2046.355\$$$

Total direct capital costs

$$DCC = C_m + C_{cw} + C_{I/P} + C_{pp} + C_{sc} + C_{HX} + C_{PV} + C_{bat} = 42373.88\$$$

Indirect capital costs

$$ICC = 0.1\times DCC = 0.1\times 42373.88 = 4237.388\$$$

Total capital costs

$$CC = DCC + ICC = 42373.88 + 4237.388 = 46611.27\$$$

*A.3.2. Operation and maintenance costs*

Membrane replacement cost

$$C_{m,repl} = 0.15 \times C_m = 0.15 \times 3603.481 = 540.522\$ \text{ / year}$$

Battery replacement cost

$$C_{bat,repl} = 0.5 \times C_{bat} = 0.5 \times 2046.355 = 2046.355\$ \text{ / } year$$

Cost of chemicals

$$C_{ch} = 365 f Q_{p,d} \times 0.018 = 365 \times 0.9 \times 7.8 \times 0.018 = 46.121\$ \text{ / } year$$

Cost of spares

$$C_{sp} = 365 f Q_{p,d} \times 0.033 = 365 \times 0.9 \times 7.8 \times 0.033 = 84.556\$ \text{ / } year$$

Cost of labor

$$C_{lb} = 365 f Q_{p,d} \times 0.03 = 365 \times 0.9 \times 7.8 \times 0.03 = 76.869\$ \text{ / } year$$

Cost of brine disposal

$$C_{bd} = 365 f Q_{p,d} \times 0.015 = 365 \times 0.9 \times 7.8 \times 0.015 = 38.434\$ \text{ / } year$$

Total annual O&M cost

$$C_{O\&M} = C_{m,repl} + C_{bat,repl} + C_{ch} + C_{sp} + C_{lb} + C_{bd} = 1809.68\$ \text{ / } year$$

*A.3.3. Total annual cost*

Amorization factor

$$a = \frac{i(1+i)^n}{(1+i)^n - 1} = \frac{0.05 \times (1+0.05)^{20}}{(1+0.05)^{20} - 1} = 0.08 year^{-1}$$

Annual fixed charges

$$C_{fixed} = aCC = 0.08 \times 46611.27 = 3740.21\$ \text{ / } year$$

Total annual cost

$$C_{total} = C_{fixed} + C_{O\&M} = 3740.21 + 1809.68 = 5549.89\$ \text{ / } year$$

*A.3.4. Water production cost*

$$WPC = \frac{C_{\text{total}}}{f Q_{p,d} 365} = \frac{5549.89}{0.9 \times 7.8 \times 365} = 2.16\$ \text{ / } m^3$$